Check for updates

Received: 21 May 2023 | Revised: 31 October 2023 | Accepted: 11 December 2023

DOI: 10.1002/cjce.25172

RESEARCH ARTICLE

THE CANADIAN JOURNAL OF CHEMICAL ENGINEERING

A kinetic model of the cycloaddition reactions between cyclopentadiene and 1,3-butadiene for synthesis of 5-vinyl-2-norbornene

Hao Li[2] | **Xue Liu**[2] | **Yan Zhang**[2] | **Yang Xiao**[3] | **Kun Cao**[1,2]

[1]State Key Laboratory of Chemical Engineering, College of Chemical and Biological Engineering, Zhejiang University, Hangzhou, China

[2]Institute of Polymerization and Polymer Engineering, Zhejiang University, Hangzhou, China

[3]Institute for Micromanufacturing and Department of Chemical Engineering, Louisiana Tech University, Ruston, Louisiana, USA

Funding information

National Key Research and Development Program of China, Grant/Award Number: 2021YFB3800702; National Natural Science Foundation of China, Grant/Award Number: 21978252; College of Engineering and Science at Louisiana Tech University

Abstract

Under high temperature and pressure, a continuous tubular reactor was successfully utilized to investigate the kinetics of 5-vinyl-2-norbornene (VNB) production. The process involved multiple cycloaddition reactions between cyclopentadiene (CPD) and 1,3-butadiene (BD). The results, spanning a wide range of operating conditions, indicate that higher temperature (180°C) and proper residence time (72 min) were conducive to efficient synthesis of VNB. The apparent kinetic parameters, including activation energies and pre-exponential factors, were acquired by fitting experimental data under integral operating conditions. The kinetic model was proven effective from a practical point of view in predicting the concentration changes of each product in the range 140 to 180°C and 30 to 80 wt.% concentration. This work provides a solid basis for the optimization of the VNB synthesis process.

KEYWORDS

1,3-butadiene, cycloaddition, cyclopentadiene, Diels–Alder reaction, kinetics, tubular reactor

1 | INTRODUCTION

5-vinyl-2-norbornene (VNB) is a key intermediate that can be readily isomerized to 5-ethylidene-2-norbornene (ENB),[1–3] one of the most important norbornene derivatives. ENB is the optimum third monomer for the production of ethylene propylene diene elastomers (EPDM).[4–6] Therefore, a further study of VNB synthesis is of critical importance. The kinetics play a key role in the investigation of reaction mechanism and process scale-up. Tubular reactors and micro-reactors are widely used in reaction mechanism research due to their real-time operation and excellent heat and mass transfer capabilities.[7–10]

At room temperature (around 25°C), cyclopentadiene (CPD) tends to dimerize and becomes enriched in dicyclopentadiene (DCPD).[11] Therefore, the production process of VNB is divided into two main steps: thermal decomposition (the reverse Diels–Alder reaction) of DCPD into CPD,[12] and the Diels–Alder reaction between CPD and 1,3-butadiene (BD).[13] The reaction mechanism of VNB production has been extensively investigated since the first report of ENB production in the 1970s.[14] The consecutive and parallel cycloaddition reactions, which occur during the production process of VNB, make thorough study of the mechanism and kinetics a challenge. Although Just et al.[15] and Fehrmann et al.[16] studied the mechanism and developed a kinetic model, no attention was paid to two kinds of key trimers, 4,4a,4b,5,8,8a,9,9a-octahydro-1H-1,4-methanofluorene (OMF) and 2-vinly-1,2,3,4,4a,5,8,8a-octahydro-1,4-methanonaphthalene (VOMN), as by-products 10 and 11 respectively in Figure 1. During the reaction process, there will be lots of DCPD reacting with BD to generate OMF, which

 © 2023 Canadian Society for Chemical Engineering.

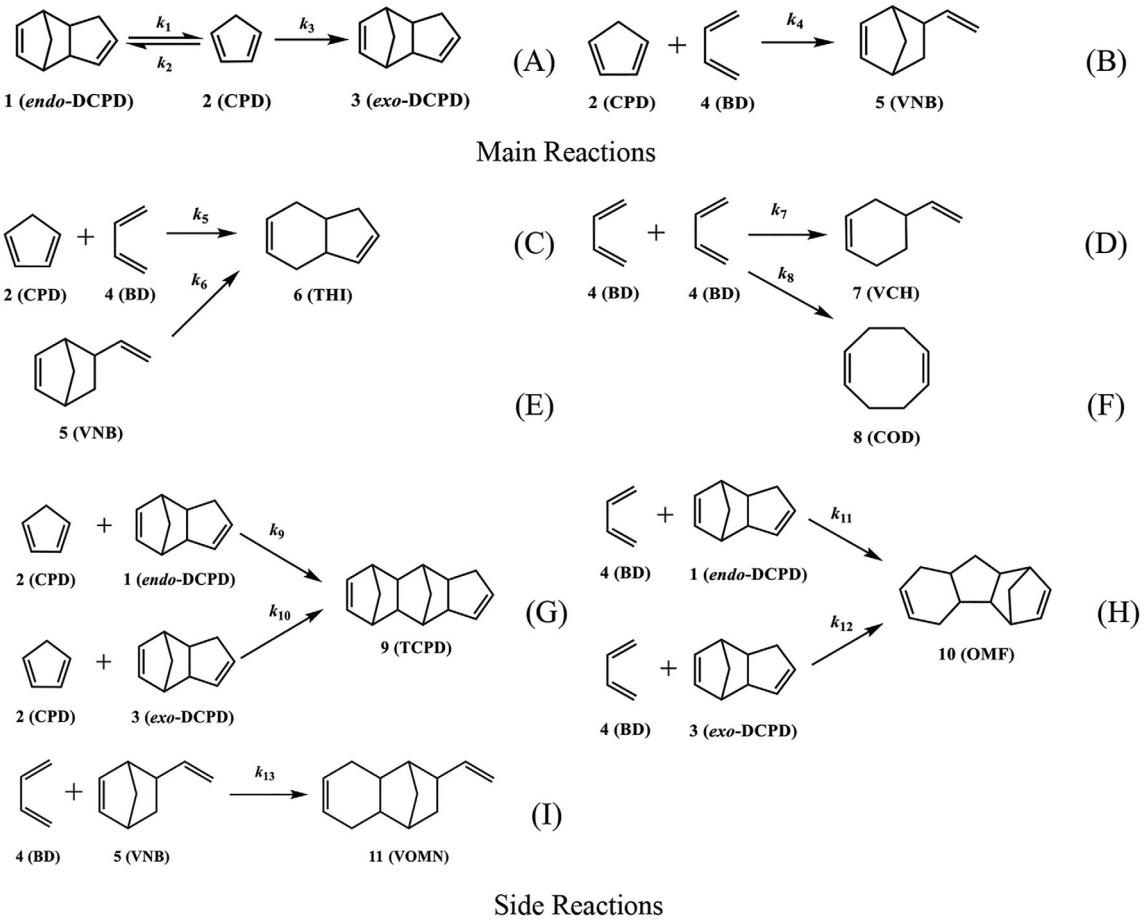


FIGURE 1 Summary of main and side reactions. BD, 1,3-butadiene; COD, 1,5-cyclooctadiene; CPD, cyclopentadiene; DCPD, dicyclopentadiene; OMF, 4,4a,4b,5,8,8a,9,9a-octahydro-1H-1,4-methanofluorene; TCPD, tricyclopentadiene; THI, 3a,4,7,7a-tetrahydroindene; VCH, 4-vinyl-cyclohexene; VNB, 5-vinyl-2-norbornene; VOMN, 2-vinly-1,2,3,4,4a,5,8,8a-octahydro-1,4-methanonaphthalene.

result in the consumption of reactants. In addition, the reaction between the target product (VNB) and reactant (BD) to generate VOMN also leads to a decrease in its concentration, which needs to be avoided as much as possible. This leads to a discrepancy of their kinetic model when compared against experimental results. Osokin[17] considered almost all possible chemical reaction pathways and thus obtained kinetic parameters for the synthesis of VNB, but no experimental validation was performed. Besides our previous work[18] demonstrating the byproduct OMF as produced by DCPD reacting with BD, Titova et al.[19] studied this side reaction and obtained its kinetic parameters.

According to prior studies, the synthesis of VNB could be described by a set of consecutive and parallel reactions shown in Figure 1.[13,15,16,18–21] In particular, Li et al.[21] confirmed that DCPD has two configurations, *exo*-DCPD and *endo*-DCPD, which is consistent with our gas chromatography (GC) and mass spectrometry (MS) analysis. Obviously, the dynamics would be more reliable if oligomerization and thermal dissociation of the two configurations were considered simultaneously.[12] Nevertheless, the polymer produced by the radical polymerization mechanism is not included in the kinetics study, due to the insignificant impact on our dynamics research proved by experiments.[18]

Furthermore, the VNB synthesis requires harsh conditions including high temperature and pressure,[15,18] due to the large matching energy gap between the orbits of dienophiles and CPD.[22–25] Because of the harsh reaction conditions, several exothermic reactions were initiated,[26] which significantly elevated the risk of runaway for the VNB synthesis process.[27,28] In 1973, the Japan Petroleum Chemical's stirred tank reactor for the production of VNB exploded, forcing a stop to production of VNB.[14]

Therefore, from both industrial and technological perspectives, it is essential to conduct more thorough research on the reaction kinetics of VNB production. In this work, we studied the cycloaddition reactions between BD and CPD under a wide range of operating conditions in a continuous tubular reactor.

19390019x, 0, Downloaded from https://onlinelibrary.wiley.com/doi/10.1002/cjce.25172 by Queens College Libraries, Wiley Online Library on [16/01/2024]. See the Terms and Conditions (https://onlinelibrary.wiley.com/terms-and-conditions) on Wiley Online Library for rules of use; OA articles are governed by the applicable Creative Commons License

2 | EXPERIMENT AND MATHEMATICAL MODEL

2.1 | Materials

The raw materials BD (99.9%) and DCPD (97.0%) were generously provided by Sinopec Shanghai Petrochemical Company Ltd. Toluene (analytical reagent, 99.0%), offered by Shanghai Lingfeng Chemical Reagent Co. Ltd, helped gradually release the heat of reaction. *N*,*N*-Diethylhydroxylamine (95.0%, inhibitor) and 4-tert-Butylcatechol (99.0%, inhibitor) were bought from J&K Scientific Ltd.

2.2 | Experiment

All experiments were performed in a specially designed continuous tubular reactor 50 m in length and having a 20 mm internal diameter. All experimental data was obtained under integral operating conditions (conversions typically >10%). Four sampling ports were installed at equal distances along the flowing direction, as shown in Figure 2. Four different residence time samples can be obtained simultaneously in a single experiment. The BD feed system and DCPD toluene solution feed system were separated. Both systems were equipped with a real-time flow monitor control system.

Samples were collected in a 2 mL sample vial after reaching steady-state and cooled quickly with an ice bath to stop the reactions for analysis. To reduce experimental deviation, at least three samples were taken at each sampling site for each experiment.

2.3 | Gas chromatography–mass spectrometry (GC–MS)/GC analysis

GC–MS analysis consists of two instruments, a gas chromatograph (Agilent 6890) and a mass selective detector (Agilent 5973 MSD), which operated in EI mode at 70 eV. An HP-MS column (HP-1, 50 m, 0.2 mm, 0.5 μm) was used. The temperature program began at an initial setpoint of 70°C, increasing at 30°C/min to 130°C, then increasing to 300°C at a rate to 10°C/min, and finally holding for 5 min at 300°C. The transfer line was held at 280°C, the ion source temperature was 230°C, and the quadrupole temperature was 150°C. The reaction products are identified in our previously published work.[18]

2.4 | Mathematical model

The dispersion model,[29,30] describing plug flow with axial dispersion, was used to fit experimental residence time distribution (RTD) data. $E(t)$ is the measured RTD function

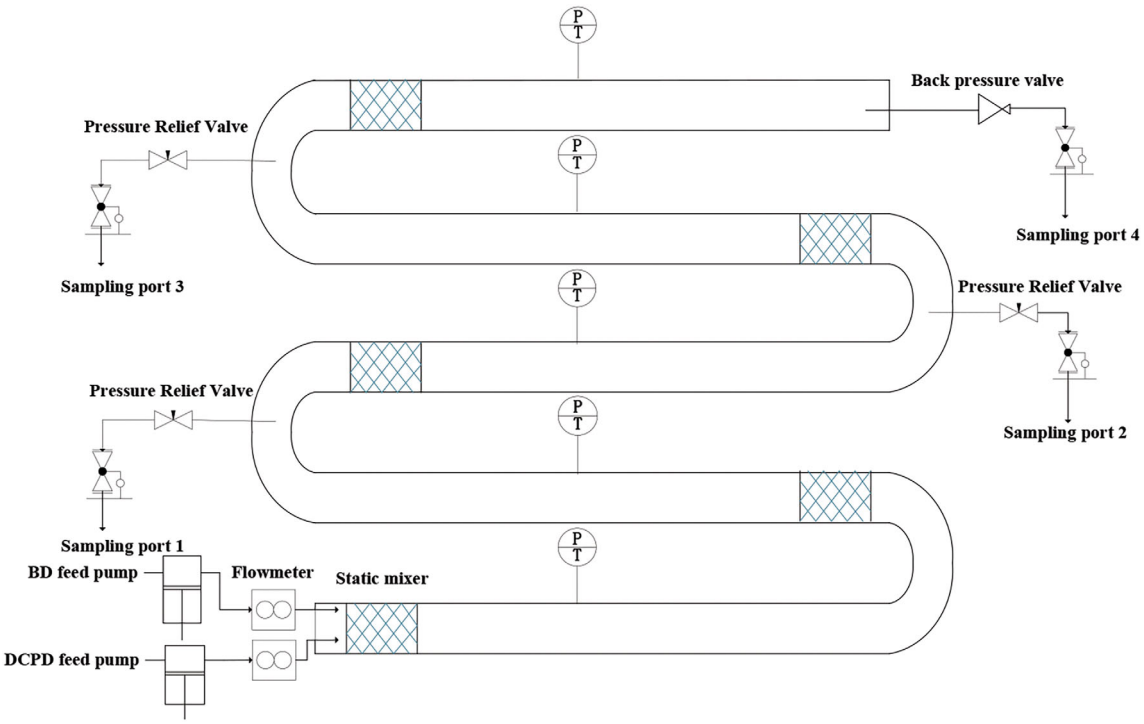


FIGURE 2 Schematic illustration of the experimental setup. BD, 1,3-butadiene; DCPD, dicyclopentadiene.

19390019x, 0, Downloaded from https://onlinelibrary.wiley.com/doi/10.1002/cjce.25172 by Queens College Libraries, Wiley Online Library on [16/01/2024]. See the Terms and Conditions (https://onlinelibrary.wiley.com/terms-and-conditions) on Wiley Online Library for rules of use; OA articles are governed by the applicable Creative Commons License

describing the time each fluid element spent in a continuous flow system. $E(t)$ dt is the fraction of fluid elements that spent time between t and $t + \mathrm{d}t$ in the flow system.

$$E(t) = \frac{c(t)}{\int_0^\infty c(t)\mathrm{d}t} \cong \frac{c(t_i)}{\sum_{i=0}^{\infty} c(t_i)\Delta t_i} \tag{1}$$

The mean residence time τ can be calculated by the following:

$$\tau = \frac{\int_0^\infty tE(t)\mathrm{d}t}{\int_0^\infty E(t)\mathrm{d}t} = \int_0^\infty tE(t)\mathrm{d}t \tag{2}$$

$$E(\theta) = \tau E(t) \tag{3}$$

$$\theta = \frac{t}{\tau} \tag{4}$$

According to Equations (5) and (6), the variance of RTD (σ^2), denoting the discrete level of RTD curve, can be expressed in a dimensionless form. The lower the variance value, the narrower the distributions. In this paper, σ^2 is calculated from the experimental data. E_z denotes the effective axial dispersion coefficient, whereas Pe denotes the Péclet number expressing the ratio of convective mass transfer and diffusive mass transfer. The larger the Pe, the closer the flow resembles a plug flow.

$$\sigma^2 = \int_0^\infty (t-\tau)^2 E(t)\mathrm{d}t = \int_0^\infty t^2 E(t)\mathrm{d}t - \tau^2 \tag{5}$$

$$\sigma(\theta)^2 = \frac{\sigma^2}{\tau^2} = 2\left(\frac{E_z}{uL}\right) = \frac{2}{\mathrm{Pe}} \tag{6}$$

$E_z/(uL)$ is a parameter of the $E(\theta)$ versus θ curve, which can be calculated from the inflection point of the distribution curve or maximum point.[31]

Under 160°C temperature, 5 MPa pressure, and 120 min residence time, the obtained experimental data was shown in Figure 3. Calculation yields mean residence time τ of 119.8 min, which is close to the experimentally expected value. The variance of RTD σ^2 was 0.41, indicating a plug flow.[32]

Individual mass balances for the CPD unit, BD unit, and toluene were developed for the tubular reactor. It was assumed that the fluid flow in the tubular reactor was an ideal plug flow, and that DCPD, BD, and toluene mixed rapidly and were homogenized in the connector.[33] According to the method recommended by Nawaf et al.,[34]

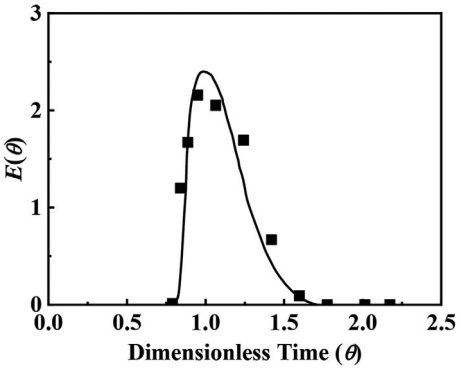


FIGURE 3 Dispersion model and experimental data at a residence time of 120 min.

the logic of the plug flow hypothesis had been proven. The Pe for all conditions involved in this work exceed 10,000, and the axial dispersion could be negligible. Cutler et al.[32] determined that random errors of experimental measurement have a more significant impact on the kinetic data than the idealization of a tubular reactor as a plug flow. Additionally, the density of the mixture solution was assumed constant during the reaction, and was replaced with the average of the initial and the final composition density under experimental conditions. This assumption is reasonable since the actual density variation during all the experiments was less than 3%.

In all reactions shown in Figure 1, the thermal decomposition of *endo*-DCPD and VNB isomerization were assumed to be first-order reactions while the rest were second-order reactions. The kinetic model of all involved reactions was as follows.

$$-\frac{\mathrm{d}C_1}{\mathrm{d}t} = k_1C_1 - k_2C_2^2 + k_9C_2C_1 + k_{11}C_1C_4 \tag{7}$$

$$\frac{\mathrm{d}C_2}{\mathrm{d}t} = 2k_1C_1 - 2k_2C_2^2 - 2k_3C_2^2 - (k_4+k_5)C_2C_4 - k_9C_2C_4 - k_{10}C_2C_3 \tag{8}$$

$$\frac{\mathrm{d}C_3}{\mathrm{d}t} = k_3C_2^2 - k_{10}C_2C_3 - k_{12}C_3C_4 \tag{9}$$

$$-\frac{\mathrm{d}C_4}{\mathrm{d}t} = (k_4+k_5)C_2C_4 + 2(k_7+k_8)C_4^2 + k_{11}C_1C_4 + k_{12}C_3C_4 + k_{13}C_4C_5 \tag{10}$$

$$\frac{\mathrm{d}C_5}{\mathrm{d}t} = k_4C_2C_4 - k_6C_5 - k_{13}C_4C_5 \tag{11}$$

$$\frac{\mathrm{d}C_6}{\mathrm{d}t} = k_6C_5 + k_5C_2C_4 \tag{12}$$

1939019x, 0, Downloaded from https://onlinelibrary.wiley.com/doi/10.1002/cjce.25172 by Queens College Libraries, Wiley Online Library on [16/01/2024]. See the Terms and Conditions (https://onlinelibrary.wiley.com/terms-and-conditions) on Wiley Online Library for rules of use; OA articles are governed by the applicable Creative Commons License

TABLE 1 The experimental conditions under various temperatures.

Run	1	2	3	4	5
Temperature (°C)	140	150	160	170	180
Pressure (MPa)	5	5	5	5	5
DCPD concentration (wt.%)	30	30	30	30	30
BD/DCPD molar ratio	0.8	0.8	0.8	0.8	0.8
Inhibitor dosage (ppm)	2000	2000	2000	2000	2000
DCPD toluene solution feed (mL · min^{-1})	99.0	98.0	96.0	95.0	93.0
BD feed (mL · min^{-1})	13.5	13.3	13.1	12.9	12.7
Re	632	672	712	751	790

Abbreviations: BD, 1,3-butadiene; CPD, cyclopentadiene; DCPD, dicyclopentadiene.

$$\frac{dC_7}{dt} = k_7 C_4^2 \tag{13}$$

$$\frac{dC_8}{dt} = k_8 C_4^2 \tag{14}$$

$$\frac{dC_9}{dt} = k_9 C_1 C_2 + k_{10} C_2 C_3 \tag{15}$$

$$\frac{dC_{10}}{dt} = k_{11} C_1 C_4 + k_{12} C_3 C_4 \tag{16}$$

$$\frac{dC_{11}}{dt} = k_{13} C_4 C_5 \tag{17}$$

The rate constant k depends on temperature as described by the Arrhenius law according to Equation (18):

$$k = A \exp\left(-\frac{E}{RT}\right) \tag{18}$$

where A is the pre-exponential factor, E is the activation energy (J/mol), R is the ideal gas law constant [8.314 J/(mol · K)], and T is the reactor temperature (K).

3 | RESULTS AND DISCUSSION

3.1 | Experimental results and model fitting

The operating conditions of the calibration experiments are shown in Table 1 and integral fits of reactions for the experimental data obtained under 140–180°C with the kinetic equations are shown in Figure 4.

MATLAB simulations were utilized to obtain the rate constants (k) via nonlinear least-squares fitting of the experimental data. The ODE45 function was implemented to solve the ordinary differential equations. The activation energy (E) and pre-exponential factor (A) were obtained by analyzing the relationship between the natural logarithm of rate constants (k) and the reciprocal of temperature ($1/T$). The resulting rate constants listed in Table 2 were then substituted into Equations (7)–(17) to calculate all product time course curves (solid lines) in Figure 4.

Table 2 reports the rate constants obtained by the nonlinear least-squares fitting of the data at fixed DCPD concentration (30 wt.%), molar ratio of BD/DCPD (0.8), and reaction pressure (5 MPa) with varying temperatures for each experiment.

The theoretical predictions under integral conditions and experimental results are presented in Figure 4. The solid lines represent simulation-generated values based on the fitting of kinetic constants obtained. The strong agreement between experimental data and predicted values proves the capability of the model to accurately predict experimental results.

However, in order to assess the adequacy of this model, the residual sum of squared errors (SSE) and standard deviation analysis, which measure the goodness-of-fit, were carried out. The values of SSE and the standard deviation (σ) were calculated using Equations (19) and (20)[31]:

$$\mathrm{SSE} = \sum_{i=1}^{n} \left(C_{i\mathrm{exp},\tau} - C_{i,\tau}\right)^2 \tag{19}$$

$$\sigma = \sqrt{\frac{\sum_1^n \delta^2}{n-1}} = \sqrt{\frac{\sum_1^n \left[\left(C_{i\mathrm{exp},\tau} - C_{i,\tau}\right)/C_{i\mathrm{exp},\tau}\right]^2}{n-1}} \tag{20}$$

where $C_{i\mathrm{exp},\tau}$ refers to the mass concentration of the experimental data and $C_{i,\tau}$ is the calculated data predicted by the model.

The SSE and standard deviation σ are shown in Table S1 of the Supplementary Information. Most of the

1939019x, 0, Downloaded from https://onlinelibrary.wiley.com/doi/10.1002/cjce.25172 by Queens College Libraries, Wiley Online Library on [16/01/2024]. See the Terms and Conditions (https://onlinelibrary.wiley.com/terms-and-conditions) on Wiley Online Library for rules of use; OA articles are governed by the applicable Creative Commons License

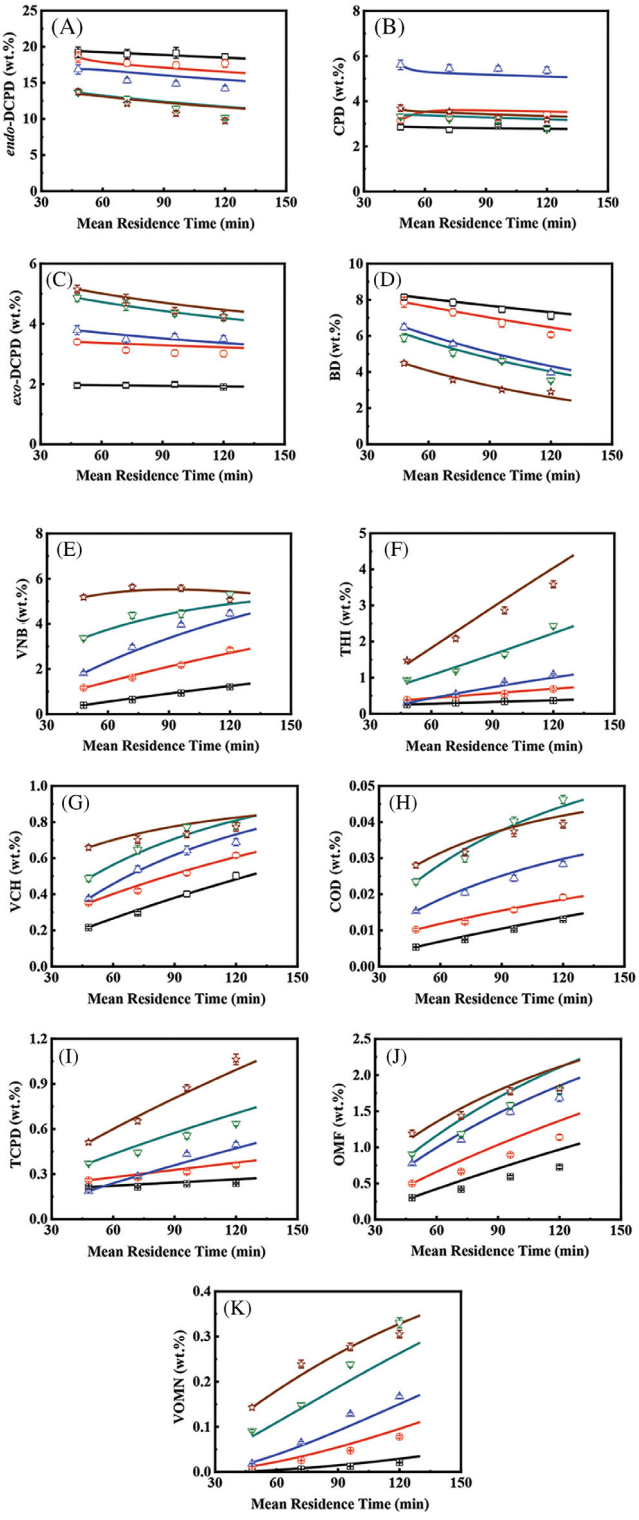


FIGURE 4 Experimental and calculated mass concentrations of components at a dicyclopentadiene (DCPD) concentration of 30 wt.%, a molar ratio of 1,3-butadiene (BD)/DCPD 0.8 and pressure of 5 MPa. The markers and solid lines represent the experimental and calculated results, respectively. (Black □: 140°C, red ○: 150°C, blue △: 160°C, green ▽: 170°C, brown ☆: 180°C.) BD, 1,3-butadiene; COD, 1,5-cyclooctadiene; CPD, cyclopentadiene; DCPD, dicyclopentadiene; OMF, 4,4a,4b,5,8,8a,9,9a-octahydro-1H-1,4-methanofluorene; TCPD, tricyclopentadiene; VCH, 4-vinyl-cyclohexene; VOMN, 2-vinly-1,2,3,4,4a,5,8,8a-octahydro-1,4-methanonaphthalene.

standard deviation values were below 0.15. The higher standard deviation values (≤0.25) were due to the relatively low concentration of VOMN. Low SSE and σ values indicate a better fit. Therefore, this model provides an excellent description of the cycloaddition of CPD with BD, since all important products are well predicted ($\sigma < 10\%$).

According to the change of conversion and selectivity with reaction temperature and residence time, shown in Figure 5, the temperature has a positive effect on the conversion, but there is no clear pattern of its effect on the selectivity of the target product, which is related to the existence of multiple consecutive and parallel reactions. The conclusion that can be drawn is that higher temperature (180°C) and proper residence time (72 min) should correspond to the efficient synthesis of VNB, in which the conversion of DCPD is 60.14%, the selectivity is 47.22%, and the yield of VNB can reach 28.40%.

3.2 | Kinetic parameters

The temperature dependence of the rate constants is shown in Figure 6. The linear fitting of ln(k) and $1/T$ was adequate. The apparent activation energy and pre-exponential factors were calculated according to the linear relationship (Table 3). The Arrhenius equation provided a good explanation of the results, per the analysis of regression coefficients (R^2). According to the apparent activation energy and pre-exponential factor, the higher temperature will promote the thermal decomposition of *endo*-DCPD and increase the concentration of CPD in solution, which is beneficial to the synthesis of VNB. However, the generation of thermodynamically stable *exo*-DCPD also increases. In addition, the apparent activation energies of the side reactions such as 4-vinyl-cyclohexene (VCH), tricyclopentadiene (TCPD), OMF, and VOMN are low, and are less sensitive to temperature changes. Although the overall concentration of some reactants decreased, the experimental results indicate that the rates of these side reactions still increase. For the other cycloaddition reactions between main reactants, the higher the reaction temperature, the faster the reaction rate, making the selectivity of VNB drop significantly after sufficient reaction. Therefore, higher temperature and proper reaction time should be more conducive to the efficient synthesis of VNB.

In addition, the enthalpy and entropy of the activation can be calculated on the basis of rate constants measured at different temperatures using Eyring–Polanyi equation[35]; the general form of the Eyring–Polanyi equation as follows:

19390019x, 0, Downloaded from https://onlinelibrary.wiley.com/doi/10.1002/cjce.25172 by Queens College Libraries, Wiley Online Library on [16/01/2024]. See the Terms and Conditions (https://onlinelibrary.wiley.com/terms-and-conditions) on Wiley Online Library for rules of use; OA articles are governed by the applicable Creative Commons License

TABLE 2 Rate constants at a dicyclopentadiene (DCPD) concentration of 30 wt.%, molar ratio of 1,3-butadiene (BD)/DCPD 0.8 and pressure of 5 MPa.

Reaction rate constants ($mol^{1-n}L^{n-1}\ s^{-1}$)[a]	Reaction temperature (°C)				
	140	150	160	170	180
k_1	$(1.01 \pm 0.53) \times 10^{-4}$	$(1.99 \pm 0.29) \times 10^{-4}$	$(4.43 \pm 0.46) \times 10^{-4}$	$(5.97 \pm 0.57) \times 10^{-4}$	$(9.85 \pm 0.73) \times 10^{-4}$
k_2	$(1.04 \pm 0.66) \times 10^{-3}$	$(1.12 \pm 0.37) \times 10^{-3}$	$(1.16 \pm 0.54) \times 10^{-3}$	$(2.96 \pm 0.63) \times 10^{-3}$	$(4.61 \pm 0.78) \times 10^{-3}$
k_3	$(1.98 \pm 0.71) \times 10^{-6}$	$(2.51 \pm 0.13) \times 10^{-6}$	$(3.20 \pm 0.32) \times 10^{-6}$	$(6.02 \pm 0.76) \times 10^{-6}$	$(8.79 \pm 0.53) \times 10^{-6}$
k_4	$(3.71 \pm 0.69) \times 10^{-5}$	$(6.04 \pm 0.36) \times 10^{-5}$	$(8.87 \pm 0.97) \times 10^{-5}$	$(1.51 \pm 0.91) \times 10^{-4}$	$(2.20 \pm 0.76) \times 10^{-4}$
k_5	$(4.59 \pm 0.98) \times 10^{-6}$	$(1.02 \pm 0.72) \times 10^{-5}$	$(2.14 \pm 0.89) \times 10^{-5}$	$(2.34 \pm 0.86) \times 10^{-5}$	$(2.52 \pm 0.68) \times 10^{-5}$
k_6	$(2.01 \pm 0.27) \times 10^{-6}$	$(3.97 \pm 0.19) \times 10^{-6}$	$(6.56 \pm 0.28) \times 10^{-6}$	$(5.30 \pm 0.25) \times 10^{-5}$	$(1.02 \pm 0.44) \times 10^{-4}$
k_7	$(3.72 \pm 0.63) \times 10^{-6}$	$(4.22 \pm 0.26) \times 10^{-6}$	$(1.08 \pm 0.78) \times 10^{-5}$	$(1.13 \pm 0.61) \times 10^{-5}$	$(1.20 \pm 0.57) \times 10^{-5}$
k_8	$(1.17 \pm 0.22) \times 10^{-7}$	$(1.38 \pm 0.18) \times 10^{-7}$	$(4.40 \pm 0.81) \times 10^{-7}$	$(7.21 \pm 0.29) \times 10^{-7}$	$(0.98 \pm 0.27) \times 10^{-6}$
k_9	$(3.00 \pm 0.35) \times 10^{-7}$	$(3.23 \pm 0.61) \times 10^{-7}$	$(3.59 \pm 0.64) \times 10^{-7}$	$(4.99 \pm 0.89) \times 10^{-7}$	$(6.02 \pm 0.22) \times 10^{-7}$
k_{10}	$(1.02 \pm 0.74) \times 10^{-5}$	$(1.21 \pm 0.59) \times 10^{-5}$	$(2.00 \pm 0.82) \times 10^{-5}$	$(3.02 \pm 0.71) \times 10^{-5}$	$(4.03 \pm 0.23) \times 10^{-5}$
k_{11}	$(5.03 \pm 0.87) \times 10^{-6}$	$(6.50 \pm 0.80) \times 10^{-6}$	$(8.81 \pm 0.15) \times 10^{-6}$	$(8.90 \pm 0.20) \times 10^{-6}$	$(9.05 \pm 0.59) \times 10^{-6}$
k_{12}	$(3.97 \pm 0.35) \times 10^{-6}$	$(1.00 \pm 0.27) \times 10^{-5}$	$(3.04 \pm 0.84) \times 10^{-5}$	$(3.98 \pm 0.11) \times 10^{-5}$	$(4.97 \pm 0.59) \times 10^{-5}$
k_{13}	$(4.98 \pm 0.68) \times 10^{-6}$	$(7.02 \pm 0.16) \times 10^{-6}$	$(9.60 \pm 0.30) \times 10^{-6}$	$(1.06 \pm 0.32) \times 10^{-5}$	$(1.20 \pm 0.40) \times 10^{-5}$

[a]The exponents are $n = 2$ for k values in reactions (2)–(5) and (7)–(13) and $n = 1$ for k values in reactions (1) and (6).

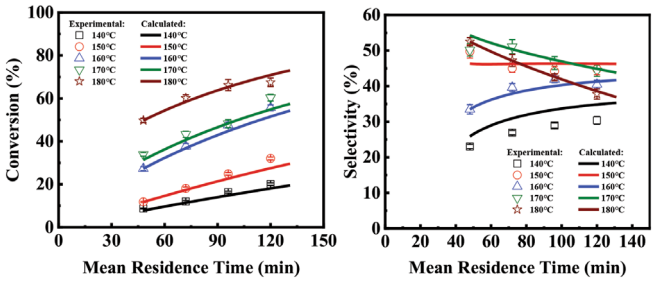


FIGURE 5 Experimental conversion of dicyclopentadiene (DCPD) and selectivity of 5-vinyl-2-norbornene (VNB) at varying conditions.

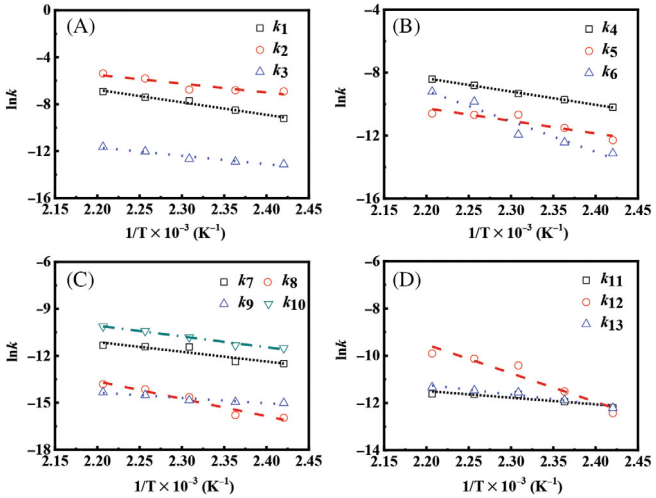


FIGURE 6 Diagram of the kinetic rate constants versus temperature.

TABLE 3 The summary of kinetic parameters.

Reaction rate constants ($mol^{1-n}L^{n-1}\ s^{-1}$)	Activation energy (kJ/mol)	Pre-exponential coefficient log A	Regression coefficient R^2
k_1	88.6	7.24	0.982
k_2	62.6	4.81	0.838
k_3	59.4	1.76	0.954
k_4	69.8	4.38	0.998
k_5	66.4	3.18	0.834
k_6	161.4	14.57	0.936
k_7	51.8	1.12	0.834
k_8	92.7	4.73	0.946
k_9	23.8	−2.97	0.926
k_{10}	57.4	2.22	0.981
k_{11}	23.5	−2.30	0.833
k_{12}	101.0	7.46	0.927
k_{13}	33.8	1.00	0.947

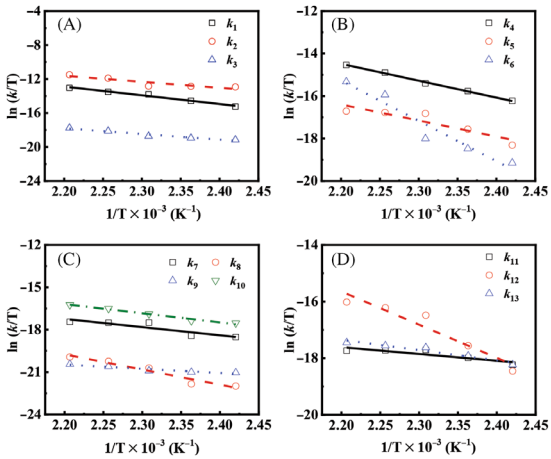


FIGURE 7 Diagram of ln (k/T) versus 1/T.

1939019x, 0, Downloaded from https://onlinelibrary.wiley.com/doi/10.1002/cjce.25172 by Queens College Libraries, Wiley Online Library on [16/01/2024]. See the Terms and Conditions (https://onlinelibrary.wiley.com/terms-and-conditions) on Wiley Online Library for rules of use; OA articles are governed by the applicable Creative Commons License

TABLE 4 The summary of activation parameters.

Reaction rate constants ($mol^{1-n}L^{n-1}\ s^{-1}$)	Activation energy ($kJ \cdot mol^{-1}$)	Enthalpy of activation ($kJ \cdot mol^{-1}$)	Entropy of activation ($J \cdot mol^{-1} \cdot K^{-1}$)
k_1	88.6	85.0	−117.8
k_2	62.6	59.0	−164.3
k_3	59.4	55.8	−222.6
k_4	69.8	66.2	−172.4
k_5	66.4	62.8	−195.7
k_6	161.4	157.8	22.6
k_7	51.8	48.2	−234.8
k_8	92.7	89.1	−165.8
k_9	23.8	24.8	−313.3
k_{10}	57.4	53.8	−213.9
k_{11}	23.5	19.9	−300.4
k_{12}	101.0	97.4	−113.4
k_{13}	33.8	30.2	−275.4

$$k = \frac{\kappa k_B T}{h} \exp\left(-\frac{\Delta G^{\neq}}{RT}\right) = \frac{\kappa k_B T}{h} \exp\left(-\frac{\Delta H^{\neq} - T\Delta S^{\neq}}{RT}\right)$$

It can be rewritten as follows:

$$\ln\frac{k}{T} = \frac{-\Delta H^{\neq}}{R} \cdot \frac{1}{T} + \ln\frac{\kappa k_B}{h} + \frac{\Delta S^{\neq}}{R}$$

where k is the rate constant, $\Delta G^{\neq}$ is the Gibbs energy of activation, $\Delta H^{\neq}$ is the enthalpy of activation, $\Delta S^{\neq}$ is the entropy of activation, κ is the transmission coefficient, k_B is the Boltzmann constant, T is the temperature, and h is the Planck constant. The plot of ln (k/T) versus $1/T$ were shown in Figure 7. The enthalpy and entropy of activation were calculated according to the linear relationship (Table 4).

TABLE 5 Comparative summary of kinetic parameters.

Ref.	Activation energy ($kJ \cdot mol^{-1}$)			Pre-exponential coefficient log A		
	This work	Data of Fehrmann et al.[16]	Data of Titova et al.[19]	This work	Data of Fehrmann et al.[16]	Data of Titova et al.[19]
Temperature range	140–180°C	120–170°C	150–200°C	140–180°C	120–170°C	150–200°C
k_1	88.6	145.5	125.6	7.24	13.36	11.20
k_2	62.6	68.2	83.5	4.81	5.69	7.86
k_3	59.4	-	-	1.76	-	-
k_4	69.8	79.3	113.4	4.38	5.79	10.31
k_{-4}	-	-	154.0	-	-	12.30
k_5	66.4	80.1	-	3.18	5.03	-
k_6	161.4	134.2	104.2	14.57	11.36	8.23
k_7	51.8	82.4	101.1	1.12	4.67	7.47
k_8	92.7	99.9	-	4.73	5.31	-
k_9	23.8	-	-	−2.97	-	-
k_{10}	57.4	-	-	2.22	-	-
k_{11}	23.5	-	121.8	−2.30	-	9.36
k_{12}	101.0	-	-	7.46	-	-
k_{13}	33.8	-	-	1.00	-	-

TABLE 6 The verification experimental conditions.

Run	6	7	8	9
Temperature (°C)	160	160	160	160
Pressure (MPa)	5	5	5	5
DCPD concentration (wt.%)	60	80	30	30
BD/CPD molar ratio	0.8	0.8	1.6	2.0
Inhibitor dosage (ppm)	2000	2000	2000	2000
DCPD toluene solution feed ($mL \cdot min^{-1}$)	85.0	79.0	85.0	80.0
BD feed ($mL \cdot min^{-1}$)	23.1	28.7	23.1	27.2
Re	795	846	817	863

Abbreviations: BD, 1,3-butadiene; CPD, cyclopentadiene; DCPD, dicyclopentadiene.

1939019x, 0, Downloaded from https://onlinelibrary.wiley.com/doi/10.1002/cjce.25172 by Queens College Libraries, Wiley Online Library on [16/01/2024]. See the Terms and Conditions (https://onlinelibrary.wiley.com/terms-and-conditions) on Wiley Online Library for rules of use; OA articles are governed by the applicable Creative Commons License

As shown in Table 4, there are differences in enthalpy and entropy changes of the reactions between CPD/BD and two configurations of DCPD. Analyzing the bonding process and product structure, the above differences are unreasonable. The reactions were coupled and interacted with each other, and only the apparent kinetic parameters could be obtained. The enthalpy and entropy calculated from the apparent kinetic parameters may deviate significantly from the actual values and are only of reference significance. Therefore, the enthalpy and entropy changes of each reaction should conduct separate studies on the corresponding reactions in subsequent research.

The partial kinetic parameters of VNB synthesis had been reported in the works of Fehrmann et al. and Titova et al.[16,19] As seen from Table 5, there are discrepancies in the kinetic parameters of varying reactions. In comparison, the number and pathways of reactions both vary. The equilibrium and isomeric reactions lead to deviations in the solutions of differential equations. Due to the influence of mass and heat transfer in varying reactors, the actual reaction rate may vary at different reaction temperatures, and the calculated apparent activation energies and pre-exponential factor are different from the values in the literature. In addition, the generation of oligomers during the actual reaction process can also have an undeniable impact on the results.

3.3 | Model validation

Using the kinetic parameters determined by fitting under integral conditions could provide a quantitative prediction of the experimental results for temperatures ranging from 140 to 180°C (Figure 4, Table 2). The apparent activation energy and pre-exponential factor shown in Table 3 were used for the model validation. The operating conditions of the validation experiments are shown in Table 6 and Figure 7. In Figure 7, the symbols represent the experimental data, while the lines represent the simulation results based on the generalized kinetic rate parameters. The predictions based on the condition-specific rate constants were in agreement with those used in the generalized equations.

Additionally, other experiments were carried out to check the accuracy and rationality of the kinetic model. For such a complex series of kinetic parameters, it is too difficult to rigorously demonstrate its authenticity one-to-one. Here, the effectiveness of the model was proved indirectly from a practical point of view.

Figure 8 displays that the simulation results (lines) predicted by the reaction kinetics model correlate well with the experimental data (markers). The model exhibits excellent fitting performance under various feed concentrations and raw material ratios, which proves the

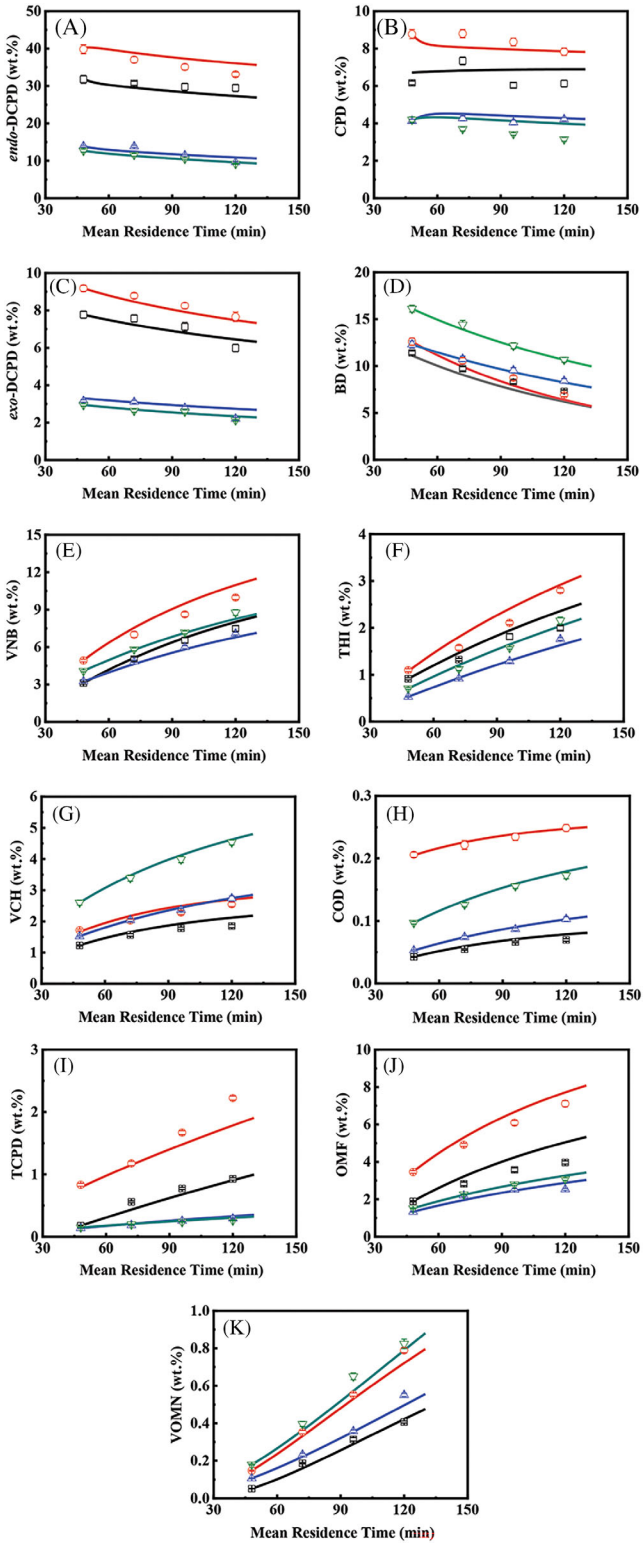


FIGURE 8 Experimental and calculated mass concentration of each product. The markers and solid lines represent the experimental and calculated results, respectively. (Black □: 60 wt.% DCPD-BD: DCPD = 0.8, red ○: 80 wt.% DCPD-BD:DCPD = 0.8, blue △: 30 wt.% DCPD-BD:DCPD = 1.6, green ▽: 30 wt.% DCPD-BD:DCPD = 2.0); BD, 1,3-butadiene; COD, 1,5-cyclooctadiene; CPD, cyclopentadiene; DCPD, dicyclopentadiene; OMF, 4,4a,4b,5,8,8a,9,9a-octahydro-1H-1,4-methanofluorene; TCPD, tricyclopentadiene; VCH, 4-vinyl-cyclohexene; VOMN, 2-vinly-1,2,3,4,4a,5,8,8a-octahydro-1,4-methanonaphthalene.

1939019x, 0, Downloaded from https://onlinelibrary.wiley.com/doi/10.1002/cjce.25172 by Queens College Libraries, Wiley Online Library on [16/01/2024]. See the Terms and Conditions (https://onlinelibrary.wiley.com/terms-and-conditions) on Wiley Online Library for rules of use; OA articles are governed by the applicable Creative Commons License

validity of the established model. The sum of square error and the standard deviation are shown in Table S2 of the Supporting Information.

4 | CONCLUSIONS

In this work, a continuous tubular reactor has been successfully applied to investigate the reaction kinetics of VNB synthesis by the cycloaddition between CPD and BD under high temperature and pressure. A detailed kinetic model was developed for a wide range of DCPD concentrations (30–80 wt.%), the molar ratio of BD/DCPD (0.8–2.0), reaction temperature (140–180°C), and pressure (5 MPa). The model was verified against the experimental data and was in agreement. Additionally, for each reaction, activation energy and pre-exponential factor were determined. The kinetic model adopts a temporary basis for scale-up design studies and further pilot-scale experiments in larger-diameter tubes.

AUTHOR CONTRIBUTIONS

Hao Li: Data curation; formal analysis; investigation; writing – original draft. **Xue Liu:** Data curation; formal analysis; investigation. **Yan Zhang:** Investigation; methodology; validation. **Yang Xiao:** Supervision; writing – review and editing. **Kun Cao:** Conceptualization; supervision; writing – review and editing.

ACKNOWLEDGEMENTS

This work was supported financially by the National Key Research and Development Program of China (No. 2021YFB3800702) and the National Natural Science Foundation of China (No. 21978252). Y. X. appreciated the start-up fund from the College of Engineering and Science at Louisiana Tech University.

CONFLICT OF INTEREST STATEMENT

The authors declare that they have no known competing financial interests or personal relationships that could have appeared to influence the work reported in this paper.

PEER REVIEW

The peer review history for this article is available at https://www.webofscience.com/api/gateway/wos/peer-review/10.1002/cjce.25172.

DATA AVAILABILITY STATEMENT

The data that support the findings of this study are available in the supplementary material of this article.

ORCID

Yang Xiao https://orcid.org/0000-0003-1705-2213

REFERENCES

[1] H. S. Kim, S. Y. Lee, H. Lee, Y. Y. Bae, S. J. Park, M. Cheong, J. S. Lee, C. H. Lee, *J. Organomet. Chem.* **2006**, *71*, 911.
[2] E. V. Bermesheva, A. I. Wozniak, I. L. Borisov, N. P. Yevlampieva, O. S. Vezo, G. O. Karpov, M. V. Bermeshev, A. F. Asachenko, M. A. Topchiy, P. S. Gribanov, M. S. Nechaev, V. V. Volkov, E. S. Finkelshtein, *Polym. Sci., Ser. C* **2019**, *61*, 86.
[3] A. H. Farquhar, M. Brookhart, A. J. M. Miller, *Polym. Chem.* **2020**, *11*, 2576.
[4] A. Malmberg, B. Löfgren, *J. Appl. Polym. Sci.* **1997**, *66*, 35.
[5] G. Leone, G. Zanchin, R. Di Girolamo, F. De Stefano, C. Lorber, C. De Rose, G. Ricci, F. Bertini, *Macromolecules* **2020**, *53*, 5881.
[6] E. E. Faingol'd, S. L. Saratovskikh, A. N. Panin, O. N. Babkina, I. V. Zharkov, N. O. Garifullin, G. V. Shilov, N. M. Bravaya, *Polymer* **2021**, *220*, 123559.
[7] C. A. Shukla, R. S. Atapalkar, A. A. Kulkarni, *Reaction Chemistry & Engineering Journal* **2020**, *5*, 736.
[8] F. Florit, V. Busini, G. Storti, R. Rota, *Chem. Eng. J.* **2019**, *373*, 792.
[9] M. Magosso, M. van den Berg, J. van der Schaaf, *Reaction Chemistry & Engineering journal* **2021**, *6*, 1574.
[10] Q. Xu, H. Fan, H. Yao, D. Wang, H. Yu, B. Chen, Z. Yu, W. Su, *Chem. Eng. J.* **2020**, *398*, 125584.
[11] R. B. Moffet, *Org. Synth.* **1952**, *32*, 41.
[12] Z. Yao, X. Xu, Y. L. Dong, X. Liu, B. Yuan, K. Wang, K. Cao, *Chem. Eng. Sci.* **2020**, *228*, 115892.
[13] Z. X. Jiang, S. Z. Guo, Z. B. Yang, H. X. Ma, *Petrochem. Technol.* **2003**, *32*, 847.
[14] Kanagawa Labor Standards Bureau, *High Pressure Gas* **1974**, *2*, 528.
[15] D. G. Just, U. Lindner, W. Pritzkow, D. M. Röllig, *Journal für Praktische Chemie/Chemiker-Zeitung* **1975**, *317*, 979.
[16] D. W. Fehrmann, M. Hampel, W. Pritzkow, D. M. Röllig, *Journal für Praktische Chemie/Chemiker-Zeitung* **1975**, *317*, 966.
[17] Y. G. Osokin, *Pet. Chem.* **2007**, *47*, 1.
[18] K. Cao, X. Liu, Y. Zhang, J. L. Shi, Y. X. Song, Z. Yao, *Ind. Eng. Chem. Res.* **2015**, *54*, 7565.
[19] L. F. Titova, Y. V. Bazhanow, M. E. Basner, A. I. Nefedova, D. N. Chaplits, N. A. Belikova, *Zh. Org. Khim.* **1982**, *18*, 710.
[20] N. Nakia, S. Iwase, Y. Ishii, M. Ogawa, *J. Jpn. Pet. Inst.* **1978**, *6*, 415.
[21] Y. H. Li, J. J. Zou, X. W. Zhang, L. Wang, Z. T. Mi, *Fuel* **2010**, *89*, 2522.
[22] N. Yoshida, H. Tanaka, F. Hirata, *J. Phys. Chem. B* **2013**, *117*, 14115.
[23] M. Molina-Espíritu, R. O. Esquivel, M. Kohout, J. C. Angulo, J. A. Dobado, J. S. Dehesa, S. LópezRosa, C. Soriano-Correa, *J. Mol. Model.* **2014**, *20*, 2361.
[24] Z. Zhang, Z. W. Peng, M. F. Hao, J. G. Gao, *Synlett* **2010**, *19*, 2895.
[25] S. B. Lee, S. H. Cho, Y. W. Park, H. K. Rhee, *Stud. Surf. Sci. Catal.* **2006**, *159*, 709.
[26] X. W. Zhang, J. Qiang, Z. Q. Xiong, J. J. Zou, W. Li, Z. T. Mi, *Chem. Res. Chin. Univ.* **2008**, *2*, 175.
[27] M. Ahmed, M. Lavin, *Plant/Oper. Prog.* **1991**, *10*, 143.
[28] T. G. Lenz, J. D. Vaughan, *J. Phys. Chem.* **1989**, *93*, 1592.
[29] H. G. Zhang, S. W. Tang, B. Liang, *Chem. Eng. J.* **2011**, *174*, 652.

1939019x, 0, Downloaded from https://onlinelibrary.wiley.com/doi/10.1002/cjce.25172 by Queens College Libraries, Wiley Online Library on [16/01/2024]. See the Terms and Conditions (https://onlinelibrary.wiley.com/terms-and-conditions) on Wiley Online Library for rules of use; OA articles are governed by the applicable Creative Commons License

[30] O. Levenspiel, *Chemical Reaction Engineering (3th Edition)*, John Wiley & Sons, New York **1999**, p. 293.
[31] S. Basha, D. Keane, K. Nolan, M. Oelgemöller, J. Lawler, J. M. Tobin, A. Morrissey, *Environ. Sci. Pollut. Res.* **2015**, *22*, 2219.
[32] A. H. Cutler, M. J. Antal, J. J. Maitland, *Ind. Eng. Chem. Res.* **1988**, *27*, 691.
[33] F. Zhang, S. Marre, A. Erriguible, *Chem. Eng. J.* **2020**, *382*, 122859.
[34] A. T. Nawaf, S. A. Gheni, A. Y. Jarullah, I. M. Mujtaba, *Energy Fuels* **2015**, *29*, 3366.
[35] H. Eyring, *J. Chem. Phys.* **1935**, *3*, 107.

SUPPORTING INFORMATION

Additional supporting information can be found online in the Supporting Information section at the end of this article.

How to cite this article: H. Li, X. Liu, Y. Zhang, Y. Xiao, K. Cao, *Can. J. Chem. Eng.* **2023**, 1. https://doi.org/10.1002/cjce.25172

1939019x, 0, Downloaded from https://onlinelibrary.wiley.com/doi/10.1002/cjce.25172 by Queens College Libraries, Wiley Online Library on [16/01/2024]. See the Terms and Conditions (https://onlinelibrary.wiley.com/terms-and-conditions) on Wiley Online Library for rules of use; OA articles are governed by the applicable Creative Commons License